

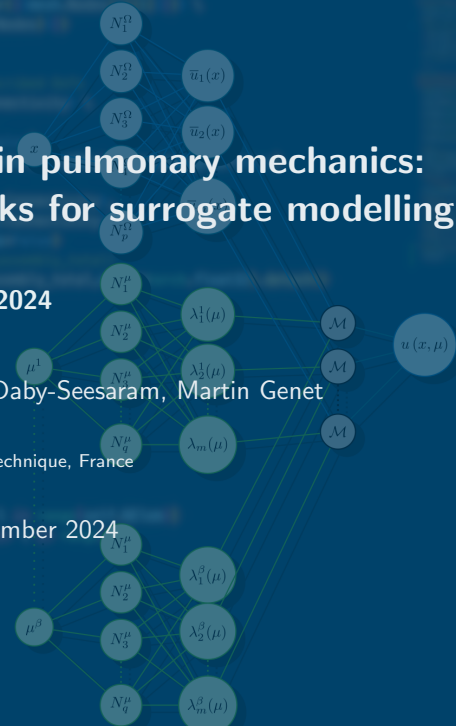
Bridging micro to macro in pulmonary mechanics: Interpretable neural networks for surrogate modelling

VPH 2024

Katerina Skardova, Alexandre Daby-Seesaram, Martin Genet

LMS, École Polytechnique, France

5th of September 2024



MOTIVATION

MULTI-SCALE LUNG MODELING

Motivation

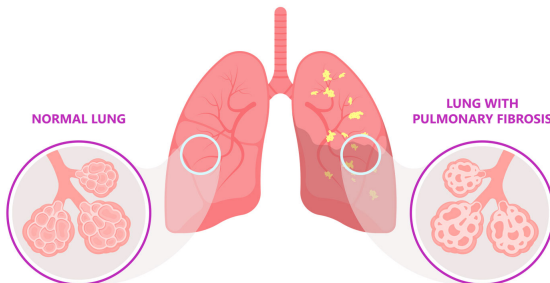
Proposed framework

Result

Conclusion & Perspectives



- Idiopathic Pulmonary Fibrosis (IPF)
- lung tissue becomes thick and stiff $\xrightarrow{\text{time}}$ permanent scarring (fibrosis)
- fibrosis effects lung tissue structure, kinematics, mechanics, ...



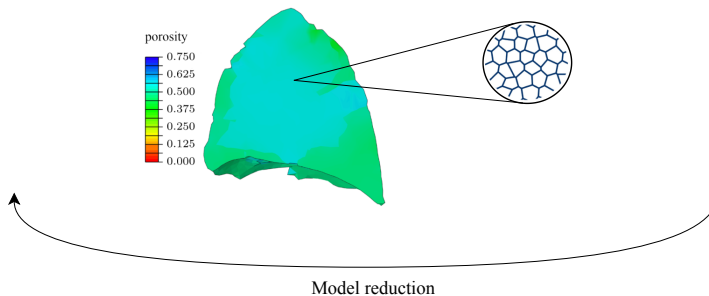
- lung model at **organ** and **alveolar** scale

MOTIVATION

MULTI-SCALE LUNG MODELING

Motivation
Proposed framework
Result
Conclusion & Perspectives

- organ spatial scale
- personalization based on image data
[Patte et al., 2022b, Patte et al., 2022a,
Laville et al., 2023,
Peyraut and Genet, 2024]
- alveolar scale model
- some of the micromechanical features
[Manoochehrtayebi et al.,]



1 FINITE ELEMENTS & NEURAL NETWORKS

2 PHYSICS-INFORMED LOSS FUNCTIONS

3 MODEL ARCHITECTURE

4 MESH ADAPTIVITY

FINITE ELEMENTS & NEURAL NETWORKS

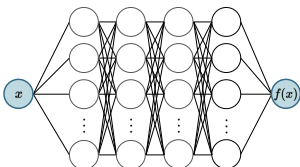
Motivation
Proposed framework
Result
Conclusion & Perspectives



- interpolation using classical FEM shape functions

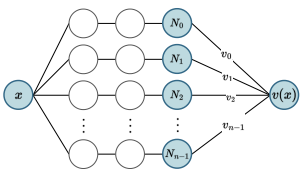
$$v(x) = \sum_{i=0}^{n-1} v_i N_i(x), \quad v_i \in \mathbb{R}, \quad i = 0, \dots, n-1$$

- physically-informed neural networks (PINNs) [Raissi et al., 2019]



- ▶ arbitrary width and depth of the network
- ▶ low interpretability of individual parameters
- ▶ need for retraining for updated setting

- Hierarchical deep-learning neural networks (HiDeNN) [Zhang et al., 2021, Zhang et al., 2022]



- coefficients v_i as parameters of neural network
- shape functions N_i constructed within the network
- strongly imposed Dirichlet boundary conditions

PHYSICS-INFORMED LOSS FUNCTION

RESIDUAL LOSS FUNCTION

- strong formulation of linear elastostatic problem

$$\text{find } \underline{u} : \begin{cases} \nabla \cdot \underline{\sigma}(\underline{u}) + \underline{f} = 0 & \text{in } \Omega, \\ \underline{n} \cdot \underline{\sigma}(\underline{u}) = \underline{t} & \text{on } \Gamma_N, \\ \underline{u} = \underline{u}_D & \text{on } \Gamma_D, \end{cases}$$

- combination of PDE residuals, used in classical PINNs [Raissi et al., 2019]

- #### ■ displacement-only setting

$$\tilde{L}_r = \frac{\lambda_1}{n_\Omega} \sum_{i=0}^{n_\Omega-1} \left(\nabla \cdot \underline{\underline{\sigma}}(\underline{u}) - \underline{\underline{f}} \right)^2 + \frac{\lambda_2}{n_{\partial\Omega}} \sum_{i=0}^{n_{\partial\Omega}-1} \left(\underline{n} \cdot \underline{\underline{\sigma}}(\underline{u}) - \underline{t} \right)^2$$

- ▶ one model
 - ▶ second derivatives
 - ▶ evaluated on Ω and Γ_N

- #### ■ displacement-stress setting

$$L_r = \frac{\lambda_1}{n_\Omega} \sum_{i=0}^{n_\Omega-1} \left(\nabla \cdot \underline{\underline{\sigma}} - \underline{f} \right)^2 + \frac{\lambda_2}{n_\Omega} \sum_{i=0}^{n_\Omega-1} \left(\underline{\underline{\sigma}}(\underline{u}) - \underline{\underline{\sigma}} \right)^2$$

- ▶ two models
 - ▶ first derivatives
 - ▶ evaluated only on Ω



PHYSICS-INFORMED LOSS FUNCTION

POTENTIAL ENERGY LOSS FUNCTION

Motivation

Proposed framework

Result

Conclusion & Perspectives









- potential energy formulation of linear elastostatic problem

$$u = \underset{\underline{u}=\underline{u}_D \text{ on } \Gamma_D}{\arg \min} \frac{1}{2} \int_{\Omega} \underline{\underline{\sigma}}(\underline{u}) : \underline{\underline{\epsilon}}(\underline{u}) - \int_{\Omega} f \underline{u} - \int_{\partial \Omega_N} t \underline{u},$$

- potential energy loss function, used in original HiDeNN [Zhang et al., 2021]

$$L_p = \frac{1}{2} \int_{\Omega} \underline{\underline{\sigma}}(\underline{u}) : \underline{\underline{\epsilon}}(\underline{u}) - \int_{\Omega} f \underline{u} - \int_{\partial \Omega_N} t \underline{u},$$



PHYSICS-INFORMED LOSS FUNCTION

WEAK FORMULATION LOSS FUNCTION

Proposed framework

■ weak formulation of linear elastostatic problem

$$\text{find } \underline{u} : \begin{cases} \underline{u} = \underline{u}_D & \text{on } \Gamma_D, \\ \int_{\Omega} \underline{\underline{\sigma}}(\underline{u}) : \underline{\underline{e}}(\underline{u}^*) - \left(\int_{\partial\Omega_N} t\underline{u}^* + \int_{\Omega} f\underline{u}^* \right) = 0, & \forall u^* \in H_1^0(\Omega). \end{cases}$$

- weak-formulation loss function, used in VPINN [Berrone et al., 2022]

$$L_w = \sum_{i=0}^{n-1} \left(\int_{\Omega} \underline{\sigma}(\underline{u}) : \underline{\epsilon}(\underline{u}_i^*) - \int_{\partial\Omega_N} \underline{t}\underline{u}_i^* - \int_{\Omega} \underline{f}\underline{u}_i^* \right)^2$$



MODEL ARCHITECTURE

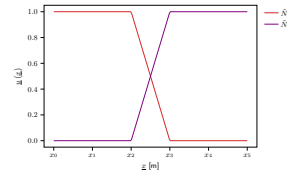
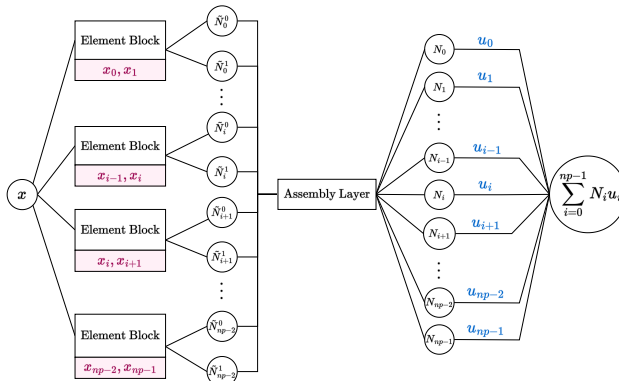
GLOBAL SHAPE FUNCTIONS

Motivation

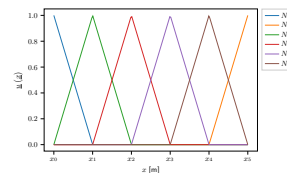
Proposed framework

Result

Conclusion & Perspectives



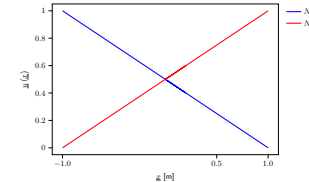
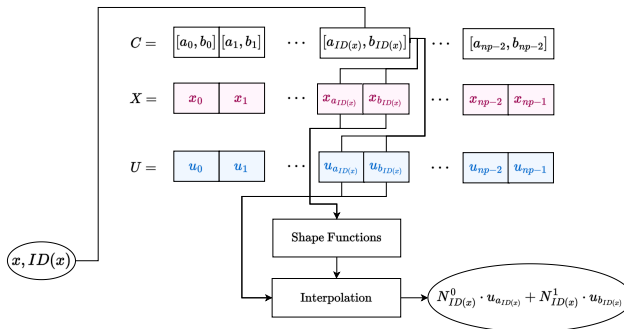
Output of one element block



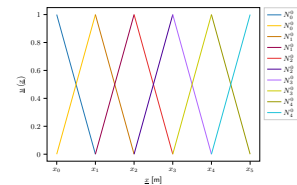
Assembled shape functions

MODEL ARCHITECTURE

LOCAL SHAPE FUNCTIONS



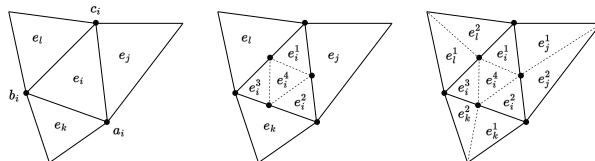
Reference element



Shape functions used for interpolation

MESH ADAPTIVITY

- both the nodal values and coordinates are parameters of the model
 - loss function differentiated w.r.t. nodal coordinates
 - r-adaptivity
 - ▶ nodal coordinates as trainable parameters
 - ▶ movement of mesh nodes based loss function derivative
 - rh-adaptivity
 - ▶ element splitting driven by movement of nodes
 - ▶ relative change of element size $>$ threshold value \implies local refinement



Red-green mesh refinement strategy [Carstensen, 2004].



1 IMPACT OF THE INTEGRATION METHOD

2 CHOICE OF LOSS FUNCTION

3 EFFECT OF MESH ADAPTIVITY



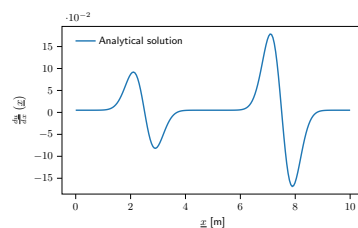
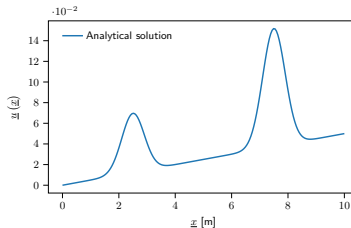
PROBLEM SETTING

- beam with two fixed ends

Motivation
Proposed framework
Result
Conclusion & Perspectives

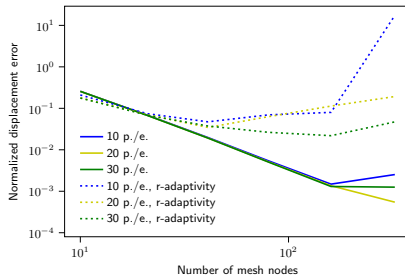
$$\frac{d}{dx} \left(AE \frac{du}{dx} \right) + b(x) = 0 \quad \text{in } \Omega = [0, L],$$
$$u(0) = 0, \quad u(L) = u_L$$

- beam section area $A = 1 \text{ mm}^2$, beam stiffness $E = 175 \text{ MP}$, $u_L = 5 \times 10^{-4} \text{ mm}$
- body force $b(x) = -\frac{(4\pi^2(x-x_1)^2 - 2\pi)}{e^{(\pi(x-x_1)^2)}} - \frac{(8\pi^2(x-x_2)^2 - 4\pi)}{e^{(\pi(x-x_2)^2)}}, x_1 = 2.5 \text{ mm}, x_2 = 7.5 \text{ mm}$

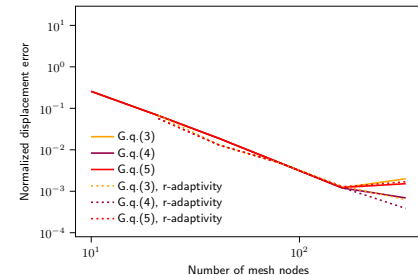


IMPACT OF THE INTEGRATION METHOD

CONVERGENCE TO ANALYTICAL SOLUTION



- trapezoidal rule
- architecture with global shape functions
- sampling points distributed uniformly



- Gaussian quadrature rule
- architecture with local shape functions
- the same number of integration points in each element

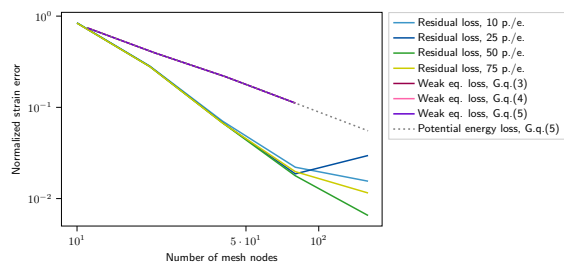
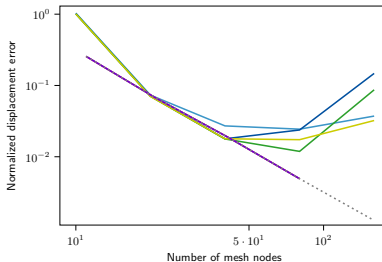


CHOICE OF LOSS FUNCTION

CONVERGENCE TO ANALYTICAL SOLUTION

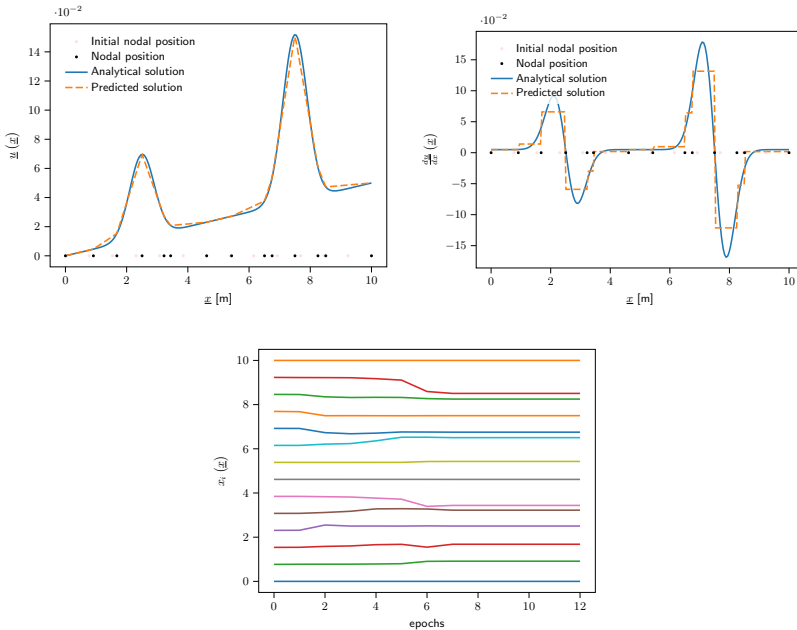


- residual loss $L_r = \frac{\lambda_1}{n_\Omega} \sum_{i=0}^{n_\Omega-1} \left(\nabla \cdot \underline{\underline{\sigma}} - \underline{f} \right)^2 + \frac{\lambda_2}{n_\Omega} \sum_{i=0}^{n_\Omega-1} \left(\underline{\underline{\sigma}}(\underline{u}) - \underline{\underline{\sigma}} \right)^2$
- potential energy loss $L_p = \frac{1}{2} \int_{\Omega} \underline{\underline{\sigma}}(\underline{u}) : \underline{\underline{\epsilon}}(\underline{u}) - \int_{\Omega} \underline{f} \underline{u} - \int_{\partial\Omega_N} \underline{t} \underline{u}$
- weak-formulation loss $L_w = \sum_{i=0}^{n-1} \left(\int_{\Omega} \underline{\underline{\sigma}}(\underline{u}) : \underline{\underline{\epsilon}}(\underline{u}_i^*) - \int_{\partial\Omega_N} \underline{t} \underline{u}_i^* - \int_{\Omega} \underline{f} \underline{u}_i^* \right)^2$



- weak-formulation loss less time efficient than potential energy loss
 - problematic balancing of terms in residual loss

EFFECT OF R-ADAPTIVITY

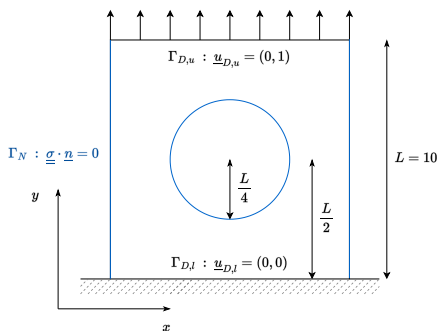


PROBLEM SETTING

Motivation
Proposed framework
Result
Conclusion & Perspectives



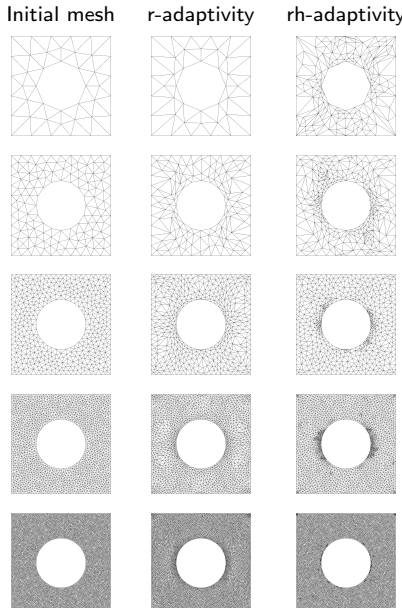
$$\begin{aligned}-\nabla \cdot \underline{\underline{\sigma}} &= 0 && \text{in } \Omega, \\ \underline{\underline{\sigma}} \cdot \underline{n} &= 0 && \text{on } \Gamma_N, \\ \underline{u} &= \underline{u}_D && \text{on } \Gamma_D,\end{aligned}$$



$$\begin{aligned}\underline{\underline{\sigma}} &= \lambda \text{tr}(\underline{\underline{\epsilon}}) \mathbb{I} + 2\mu \underline{\underline{\epsilon}} \\ \underline{\underline{\epsilon}} &= \frac{1}{2} \left(\nabla \underline{u} + (\nabla \underline{u})^T \right) \\ \lambda &= 1.25, \mu = 1.0\end{aligned}$$

MESH ADAPTIVITY

Motivation
Proposed framework
Result
Conclusion & Perspectives

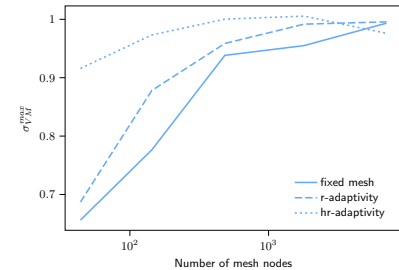
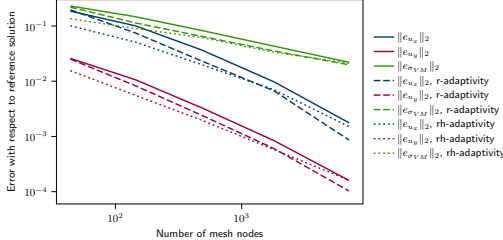


- architecture with local shape functions
- potential energy loss function

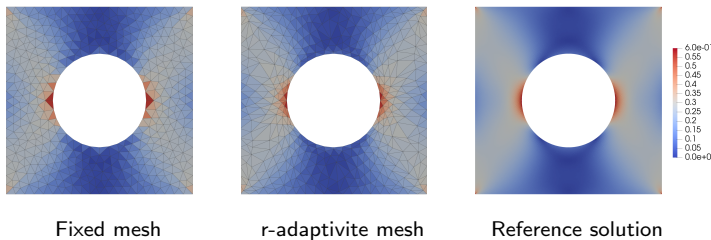
- multi-level training strategy
 - ▶ coarse to fine mesh resolution
 - ▶ straightforward initialization thanks to interpretability
 - ▶ faster / more robust training

MESH ADAPTIVITY

■ convergence to reference solution



■ von Mises stress



Motivation

Proposed framework

Result

Conclusion & Perspectives



CONCLUSION & PERSPECTIVE



- advantages of the architecture
 - ▶ strongly prescribed Dirichlet boundary conditions
 - ▶ training with fixed mesh / r-adaptivity / rh-adaptivity
 - ▶ straightforward transfer of knowledge from pre-trained model
 - extension to parametric PDEs
 - ▶ *Hybridising standard reduced-order modelling methods with interpretable sparse neural networks for real-time patient specific lung simulations*
Alexandre Daby-Seesaram, (Wed Sep 4, 2024, 2:00 PM - 2:15 PM)
 - parametrization of simplified lung microstructure

This work was supported by Bertip EUR (ANR 18EURE0002).



Bibliography

-  Berrone, S., Canuto, C., and Pintore, M. (2022). Solving PDEs by variational physics-informed neural networks: an a posteriori error analysis. *ANNALI DELL'UNIVERSITA' DI FERRARA*, 68(2):575–595.
 -  Carstensen, C. (2004). An Adaptive Mesh-Refining Algorithm Allowing for an H1 StableL2 Projection onto Courant Finite Element Spaces. *Constructive Approximation*, 20(4):549–564.
 -  Laville, C., Fetita, C., Gille, T., Brillet, P.-Y., Nunes, H., Bernaudin, J.-F., and Genet, M. (2023). Comparison of optimization parametrizations for regional lung compliance estimation using personalized pulmonary poromechanical modeling. *Biomechanics and Modeling in Mechanobiology*, 22(5):1541–1554.
 -  Manoochehrtayebi, M., Bel-Brunon, A., and Genet, M. Micro-poro-mechanics: formulation and compared analysis with macro-poro-mechanics. *In preparation*.
 -  Patte, C., Brillet, P.-Y., Fetita, C., Bernaudin, J.-F., Gille, T., Nunes, H., Chapelle, D., and Genet, M. (2022a). Estimation of regional pulmonary compliance in idiopathic pulmonary fibrosis based on personalized lung poromechanical modeling. *Journal of Biomechanical Engineering*, 144(9):091008.
 -  Patte, C., Genet, M., and Chapelle, D. (2022b). A quasi-static poromechanical model of the lungs. *Biomechanics and Modeling in Mechanobiology*, 21(2):527–551.
 -  Peyraut, A. and Genet, M. (2024). A model of mechanical loading of the lungs including gravity and a balancing heterogeneous pleural pressure. *Biomechanics and Modeling in Mechanobiology*.
 -  Raissi, M., Perdikaris, P., and Karniadakis, G. E. (2019). Physics-informed neural networks: A deep learning framework for solving forward and inverse problems involving nonlinear partial differential equations. *Journal of Computational physics*, 378:686–707.
 -  Zhang, L., Cheng, L., Li, H., Gao, J., Yu, C., Domel, R., Yang, Y., Tang, S., and Liu, W. K. (2021). Hierarchical deep-learning neural networks: finite elements and beyond. *Computational Mechanics*, 67:207–230.
 -  Zhang, L., Lu, Y., Tang, S., and Liu, W. K. (2022). HiDeNN-TD: reduced-order hierarchical deep learning neural networks. *Computer Methods in Applied Mechanics and Engineering*, 389:114414.